Eur. Phys. J. C 24, 413–424 (2002)
Digital Object Identifier (DOI) 10.1007/s10052-002-0952-8

THE EUROPEAN PHYSICAL JOURNAL C

Transverse spin effects in diffractive hadron leptoproduction

S.V. Goloskokov[a]

Bogoliubov Laboratory of Theoretical Physics, Joint Institute for Nuclear Research, 141980 Dubna, Moscow region, Russia

Received: 19 February 2002 / Revised version: 19 March 2002 /
Published online: 22 May 2002 –

Abstract. We consider double spin asymmetries for longitudinally polarized leptons and transversely polarized protons in diffractive vector meson and $Q\bar{Q}$ production at high energies within the two-gluon model. The connection of the two-gluon approach with skewed gluon distributions is discussed. The asymmetry predicted for meson production is quite small. The A_{lT} asymmetry for $Q\bar{Q}$ production contains two independent terms which are large and can be used to obtain information on the polarized skewed gluon distributions in the proton.

1 Introduction

The study of the hadron structure is a fundamental problem of modern physics. One of the important objects here is the parton distribution in a nucleon. The cross section of inclusive hadron production is expressed in terms of ordinary parton distributions where partons have the same momenta. More general structures in a nucleon can be studied in deeply virtual Compton scattering or in diffractive hadron leptoproduction. In fact, the kinematics of these processes requires a non-zero longitudinal momentum ζp carried by the two-parton system. As a result, the parton momenta cannot be equal, and such reactions are expressed in terms of skewed parton distributions (SPD) [1,2]. The factorization of the amplitude of diffractive hadron production into a hard subprocess and a soft proton matrix element – SPD – has been shown in [3]. The diffractive charm $Q\bar{Q}$ production and J/Ψ production are determined by the gluon SPD $\mathcal{F}_\zeta(x)$, because the charm component in the proton is small. The processes with light quarks are predominated at small Bjorken $x \leq 0.1$ by the pomeron exchange which can be associated with a two-gluon state [4]. Both quark and gluon SPD will contribute here for $x > 0.1$.

The sensitivity of diffractive lepto- and photoproduction to the gluon density in the proton gives an excellent tool to test these structure functions. Intensive experimental studies of diffractive processes were performed in DESY (see e.g. [5–8] and references therein). The longitudinal double spin asymmetry in vector meson production has been analyzed in [9]. A theoretical investigation of the diffractive vector meson production was conducted on the basis of different models in which the sensitivity of the experimental observables to polarized parton distributions was studied. Within the two-gluon exchange model, the typical scale $\bar{Q}^2 = (Q^2 + M_V^2)/4$ was found for vector mesons production [10,11]. The cross sections of light and heavy meson production plotted versus this variable looks similar [12]. In [13–15] the cross section for longitudinal and transverse photon polarization was analyzed. It was shown that a longitudinally polarized photon gives a predominant contribution to the cross section for $Q^2 \to \infty$. The cross section with transverse photon polarization is suppressed as a power of Q. An investigation of the vector meson production within the SPD approach was performed by many authors (see e.g. [16,17]). Within the SPS approach, one can study simultaneously the imaginary and real parts of the diffractive amplitudes. In [18], the double spin asymmetry for longitudinal lepton and proton polarization in J/Ψ production was estimated. The contribution with transversely polarized photons and a vector meson is important for a spin observable like the A_{ll} asymmetry. Unfortunately, for the light meson production, this higher twist transition amplitude is not well defined because of the infrared singularities present [19].

Another possibility to study SPD in the proton is based on the quark pair leptoproduction. A theoretical analysis of the diffractive $Q\bar{Q}$ production which can be observed as two jet events in lepton–proton interaction was carried out e.g. in [20–23]. It was shown that the cross sections of diffractive quark–antiquark production are expressed in terms of gluon distributions as in the case of vector meson production. However, the scale variable in the structure function is here determined by the transverse momentum of a produced quark. Spin effects in a diffractively produced quark–antiquark pair for longitudinally polarized lepton and proton were discussed in [24] where the diffractive contribution to the g_1 structure function was calculated.

Thus, the diffractive reactions should play a key role in the study of the gluon structure of the proton at small x. In the case of polarized particles, the spin-dependent gluon distributions can be investigated. Previously, spin asym-

[a] e-mail: goloskkv@thsun1.jinr.ru

metries for longitudinally polarized particles were mainly analyzed. In future, this will be an excellent possibility to study spin effects with a transversely polarized target at HERMES. Numerous proposals for possible experiments with this target were discussed in [25]. Such experiments should shed light on the polarized parton distributions which are responsible for the transverse spin effects in the hadron.

In this paper we consider double spin asymmetries for longitudinally polarized leptons and transversely polarized protons in diffractive vector meson and $Q\bar{Q}$ production at high energies. Some preliminary results in this field were published in [26]. The two-gluon exchange model with the spin-dependent gg–proton coupling is used. This means that our results should be applicable for reactions with heavy quarks which are determined by the gluons exchange. For processes with light quarks our predictions should be valid at small x (e.g. $x \leq 0.1$). The cross section of hadrons leptoproduction can be decomposed into leptonic and hadronic tensors and the amplitude of hadron production through the $\gamma^\star gg$ transition to the vector meson or $Q\bar{Q}$ states. After describing the kinematics of the process in Sect. 2, we analyze the structure of the leptonic and hadronic tensors in Sect. 3. In Sect. 4, we calculate the polarized cross section of vector meson leptoproduction. The connection of the two-gluon approach with skewed gluon distributions is discussed, too. Similar results for diffractive $Q\bar{Q}$ production are presented in Sect. 5. The numerical results for the diffractive vector meson and production at HERMES and COMPASS energies and our prediction for the $A_{l\mathrm{T}}$ asymmetry can be found in Sects. 6 and 7. We finish with concluding remarks in Sect. 8.

2 Kinematics of diffractive hadron leptoproduction

Let us study the diffractive hadron production in lepton–proton reactions,

$$l + p \to l + p + H, \tag{1}$$

at high energies in a lepton–proton system. The hadron state H in this reaction can contain a vector meson or a $Q\bar{Q}$ system which can be detected as two final jets. The reaction (1) can be described in terms of the kinematic variables which are defined as follows:

$$q^2 = (l - l')^2 = -Q^2, \quad t = r_P^2 = (p - p')^2, \quad y = \frac{p \cdot q}{l \cdot p},$$
$$x = \frac{Q^2}{2p \cdot q}, \quad x_P = \frac{q \cdot (p - p')}{q \cdot p}, \quad \beta = \frac{x}{x_P}, \tag{2}$$

where l, l' and p, p' are the initial and final lepton and proton momenta, respectively, Q^2 is the photon virtuality, and r_P is the momentum carried by the pomeron. The variable β is used in $Q\bar{Q}$ production. In this case the effective mass of a produced quark system is equal to $M_X^2 = (q + r_P)^2$ and can be quite large. The new variable $\beta = x/x_P \sim Q^2/(M_X^2 + Q^2)$ which appears in this case can vary from 0 to 1. For diffractive vector meson production, $M_X^2 = M_V^2$ and $\beta \sim 1$ for large Q^2. From the mass-shell equation for the vector meson momentum $K_V^2 = (q + r_P)^2 = M_V^2$, we find that for these reactions

$$x_P \sim \frac{m_V^2 + Q^2 + |t|}{sy}, \tag{3}$$

and this is small at high energies. This variable is not fixed for $Q\bar{Q}$ production.

We use the light-cone variables that are determined by $a_\pm = a_0 \pm a_z$. In these variables, the scalar product of two 4-vectors looks like

$$a \cdot b = \frac{1}{2}(a_+ b_- + a_- b_+) - \vec{a}_\perp \vec{b}_\perp,$$

where $\vec{a}_\perp$ and $\vec{b}_\perp$ represent the transverse parts of the momenta. In the calculation, the center of mass system is used where the momenta of the initial lepton and proton are going along the z axis and have the form

$$l = \left(p_+, \frac{\mu^2}{p_+}, \vec{0}\right), \quad p = \left(\frac{m^2}{p_+}, p_+, \vec{0}\right). \tag{4}$$

Here μ and m are the lepton and proton mass. The energy of the lepton–proton system then reads $s \sim p_+^2$.

The momenta are carried by the photon and the pomeron and can be written as follows:

$$q = \left(y p_+, -\frac{Q^2}{p_+}, \vec{q}_\perp\right), \quad |q_\perp| = \sqrt{Q^2(1-y)};$$
$$r_P = \left(-\frac{|t|}{p_+}, x_P p_+, \vec{r}_\perp\right), \quad |r_\perp| = \sqrt{|t|(1-x_P)}. \tag{5}$$

We can determine the spin vectors with positive helicity of the lepton and the proton by

$$s_l = \frac{1}{\mu}\left(p_+, -\frac{\mu^2}{p_+}, \vec{0}\right), \quad s_l^2 = -1, \quad s_l \cdot l = 0;$$
$$s_p = \frac{1}{m}\left(\frac{m^2}{p_+}, -p_+, \vec{0}\right), \quad s_p^2 = -1, \quad s_p \cdot p = 0. \tag{6}$$

The polarization vector for a transversely polarized target can be written in the form

$$s_p^\perp = (0, 0, \vec{s}_\perp), \quad \vec{s}_\perp^{\,2} = 1. \tag{7}$$

3 Structure of leptonic and hadronic tensors

3.1 Leptonic tensor

The structure of the leptonic tensor is quite simple [27], because the lepton is a pointlike object:

$$\mathcal{L}^{\mu\nu}(s_l) = \sum_{\text{spin } s_f} \bar{u}(l', s_f)\gamma^\mu u(l, s_l)\bar{u}(l, s_l)\gamma^\nu u(l', s_f)$$
$$= \mathrm{Tr}\left[(\not{l}' + \mu)\frac{1 + \gamma_5 \not{s}_l}{2}\gamma^\nu(\not{l}' + \mu)\gamma^\mu\right]. \tag{8}$$

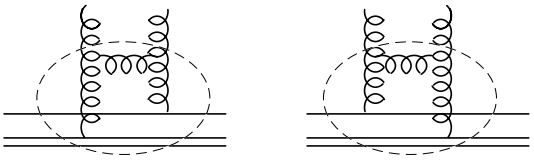

Fig. 1. Graphs which give the leading Log contribution to the ggp vertex in α^2 order

Here l and l' are the initial and final lepton momenta, and s_l is a spin vector of the initial lepton determined in (6).

The sum and difference of the cross sections with parallel and antiparallel longitudinal polarization of a proton and a lepton are expressed in terms of the spin-averaged and spin-dependent hadron and lepton tensors. The latter is determined by the relation

$$\mathcal{L}^{\mu\nu}(\pm) = \frac{1}{2}\left(\mathcal{L}^{\mu\nu}\left(+\frac{1}{2}\right) \pm \mathcal{L}^{\mu\nu}\left(-\frac{1}{2}\right)\right), \qquad (9)$$

where $\mathcal{L}^{\mu;\nu}(\pm 1/2)$ are the tensors with helicity of the initial lepton equal to $\pm 1/2$. The tensors (9) look like

$$\begin{aligned}\mathcal{L}^{\mu\nu}(+) &= 2(g^{\mu\nu} l\cdot q + 2l^\mu l^\nu - l^\mu q^\nu - l^\nu q^\mu),\\ \mathcal{L}^{\mu\nu}(-) &= 2\mathrm{i}\mu\epsilon^{\mu\nu\delta\rho} q_\delta (s_l)_\rho. \end{aligned} \qquad (10)$$

3.2 Proton–two-gluon coupling and hadron tensor

The $Q\bar{Q}$ system which appears in the final state or passes into the vector meson in reaction (1) can be produced in two ways. The first one is the photon interaction with the $Q\bar{Q}$ state from the proton. This contribution can be connected with the quark distribution in a nucleon. The other contribution is determined by the photon–gluon fusion which produces the $Q\bar{Q}$ system. The quark pair must be in a color singlet state to produce the vector meson. This means that the gluon state should be colorless too and contains two gluons at least. We are working in the low x region where the gluon contribution predominates. It is associated with the pomeron that describes diffractive processes at high energies. In QCD-inspired models, the pomeron is usually represented as a two-gluon object.

Properties of the gluon structure functions are determined by the non-perturbative effects inside the proton. We shall analyze only the matrix structure of two-gluon coupling with the proton within the quark–diquark model [28] where the proton is composed of a quark and a diquark. Composite scalar and vector diquarks provide an effective description of non-perturbative effects in the gluon–proton interaction. The vector diquark produces spin-flip effects in the proton coupling with the gluon.

It has been shown in [29] that the leading contribution like $\alpha_s\left[\alpha_s \ln(1/x)\right]^n$ to the pomeron is determined by the gluon ladder graphs. In the $[\alpha_s]^2$ order we have in the model the two ladder graphs shown in Fig. 1 with $\alpha_s^2 \ln(1/x)$ behavior. We include in the gluons coupling with the proton the gluon ladder, except for two upper t-channel gluons in Fig. 1. This coupling is shown in the graphs of Fig. 1 by the blob. In what follows, we shall calculate the imaginary part of the pomeron contribution to the scattering amplitude which dominates in the high-energy region. This contribution is equivalent to the t-channel cut in the gluon-loop graphs. In the diquark model, the following structures in the coupling appear:

$$\begin{aligned} V^{\alpha\beta}_{pgg}(p,t,x_P,l_\perp) &= B(t,x_P,l_\perp)(\gamma^\alpha p^\beta + \gamma^\beta p^\alpha)\\ &+ \frac{\mathrm{i}K(t,x_P,l_\perp)}{2m}(p^\alpha \sigma^{\beta\gamma} r_\gamma + p^\beta \sigma^{\alpha\gamma} r_\gamma)\\ &+ \mathrm{i}D(t,x_P,l_\perp)\epsilon^{\alpha\beta\delta\rho} p_\delta \gamma_\rho \gamma_5 + \cdots \end{aligned} \qquad (11)$$

Here m is the proton mass. In the matrix structure (11) we wrote only the terms with the maximal powers of a large proton momentum p. The structure functions in (11) are dependent on the transverse part of the gluon momentum $l_\perp$. The first two terms of the vertex (11) are symmetric in the gluon indices α, β. The structure proportional to $B(t,\cdots)$ determines the spin-non-flip contribution. The term $\propto K(t,\cdots)$ leads to the transverse spin-flip at the vertex. The asymmetric structure in (11) is proportional to $D\gamma_\rho\gamma_5$ and can be associated with ΔG. It should give a visible contribution to the double spin longitudinal asymmetry A_{ll}. We do not consider this structure here and concentrate on the transverse effects in the proton. In a QCD-based diquark model of the proton, the first two terms in (11) were estimated in the proton–proton scattering amplitude for moderate momentum transfer [30]. At small momentum transfer, such a model calculation is not possible, and we do not know explicitly the functions B, K, $\cdots$ in (11). Note that a coupling similar to (11) was found in high-energy quark–quark scattering when large-distance effects were considered in the gluon loops [31].

In what follows, we analyze the $\gamma^* gg \to Q\bar{Q}$ transition amplitude. The typical momentum of quarks in this case is proportional to the photon momentum q. In the Feynman gauge, we can decompose the $g_{\mu\nu}$ tensors from t-channel gluons into longitudinal and transverse parts [29]:

$$g^{\alpha\alpha'} = g_l^{\alpha\alpha'} + g_\perp^{\alpha\alpha'} \quad \text{with } g_l^{\alpha\alpha'} \sim \frac{q^\alpha p^{\alpha'}}{(pq)}. \qquad (12)$$

The product of the $g_l^{\alpha\alpha'}$ tensors by the two-gluon coupling of the proton can be written in the form

$$\begin{aligned} &g_l^{\alpha'\alpha} g_l^{\beta'\beta} V^{\alpha\beta}_{pgg}(p,t,x_P,l_\perp) \qquad (13)\\ &\propto p^{\alpha'} p^{\beta'}\left[\frac{\not{q}}{(pq)} B(t,x_P,l_\perp) + \frac{\mathrm{i}K(t,x_P,l_\perp)}{2m(pq)}\sigma^{\beta\gamma} q_\beta r_\gamma\right]. \end{aligned}$$

The structure proportional to D is asymmetric in the gluon indices. It will contribute only in the case when one of the gluon tensors in (13) has a transverse component. It can be seen that the structure in square brackets in (13) is related directly to the definitions of the skewed gluon distribution (see e.g. [1]). So, one can conclude that after integration over the gluon transverse momentum $l_\perp$, we should have the connections:

$$\mathcal{F}^g_\zeta(\zeta,t) \propto \int \mathrm{d}^2 l_\perp B(t,\zeta = x_P, l_\perp)\phi(l_\perp,\cdots),$$

$$\mathcal{K}^g_\zeta(\zeta,t) \propto \int \mathrm{d}^2 l_\perp K(t,\zeta=x_P,l_\perp)\phi(l_\perp,\cdots), \quad (14)$$

and B and K are non-integrated gluon distribution functions which describe spin-averaged and transverse spin effects in the proton. The universal function ϕ in (14) will be found later. In future calculations, we use the $g^{\alpha\alpha'}$ tensor without its decomposition into longitudinal and transverse parts.

The hadronic tensor is given by

$$W^{\alpha\alpha';\beta\beta'}(s_p) = \sum_{\text{spin } s_f} \bar{u}(p',s_f)V^{\alpha\alpha'}_{pgg}(p,t,x_P,l) \times u(p,s_p)\bar{u}(p,s_p)V^{\beta\beta'+}_{pgg}(p,t,x_P,l')u(p',s_f), \quad (15)$$

and is determined by a trace similar to (8). The spin-averaged and spin-dependent hadron tensors are defined by

$$W^{\alpha\alpha';\beta\beta'}(\pm) = \frac{1}{2}(W^{\alpha\alpha';\beta\beta'}(+s_p) \pm W^{\alpha\alpha';\beta\beta'}(-s_p)). \quad (16)$$

This form is written for an arbitrary spin vector s_p and can be used as well for transversely as for longitudinally polarized target. In the last case, the contribution of the D structure should be considered. For the leading term of the spin-averaged structure $W(+)$ for the ansatz (11) we find

$$W^{\alpha\alpha';\beta\beta'}(+) = 16 p^\alpha p^{\alpha'} p^\beta p^{\beta'} \left(|B|^2 + \frac{|t|}{m^2}|K|^2\right). \quad (17)$$

Note that we omit for simplicity, here and in what follows, the arguments of the B and K functions unless these are necessary. However, we should remember that the amplitudes B and K depend on l, otherwise the complex conjugate quantities $B^\star$ and $K^\star$ are functions of l'. The obtained equation for the spin-averaged tensor coincides in form with the cross section of the proton off the spinless particle (e.g. a meson). In fact, the meson–proton helicity-non-flip and helicity-flip amplitudes can be written in terms of the invariant functions $\tilde{B}$ and $\tilde{K}$ which describe spin-non-flip and spin-flip effects:

$$F_{++}(s,t) = \mathrm{i}s[\tilde{B}(t)]f(t); \quad F_{+-}(s,t) = \mathrm{i}s\frac{\sqrt{|t|}}{m}\tilde{K}(t)f(t), \quad (18)$$

where $f(t)$ is determined by the pomeron coupling with the meson. The functions $\tilde{B}$ and $\tilde{K}$ are defined by integrals like (14). The cross section is written in the form

$$\frac{\mathrm{d}\sigma}{\mathrm{d}t} \sim \left[|\tilde{B}(t)|^2 + \frac{|t|}{m^2}|\tilde{K}(t)|^2\right] f(t)^2. \quad (19)$$

The term proportional to $\tilde{B}$ represents the standard pomeron coupling that leads to the non-flip amplitude. The $\tilde{K}$ function is the spin-dependent part of the pomeron coupling which produces in our case the spin-flip effects non-vanishing at high energies. The models [30,32] predict a value of the single spin transverse asymmetry of about 10% for $|t| \sim 3\,\mathrm{GeV}^2$ which is of the same order of magnitude as that observed experimentally [33]. It has been found in [30,32] that the ratio $|\tilde{K}|/|\tilde{B}| \sim 0.1$ and that it has a weak energy dependence. The weak energy dependence of spin asymmetries in exclusive reactions is not in contradiction with experiment [32,34].

The spin-dependent part of the hadron tensor can be written as

$$W^{\alpha\alpha';\beta\beta'}(-) = S_0^{\alpha\alpha';\beta\beta'} + S_r^{\alpha\alpha';\beta\beta'} + A_t^{\alpha\alpha';\beta\beta'}. \quad (20)$$

The functions S are symmetric in the α,α' and β,β' indices; we have

$$S_0^{\alpha\alpha';\beta\beta'} = 8\mathrm{i}\frac{BK^* - B^*K}{m} p^\beta p^{\beta'} \Gamma^{\alpha\alpha'} \quad (21)$$

and

$$S_r^{\alpha\alpha';\beta\beta'} = 2\mathrm{i}\frac{B^*K}{m}\left(p^\alpha (r_P)^{\alpha'} + p^{\alpha'}(r_P)^\alpha\right)\Gamma^{\beta\beta'} - 2\mathrm{i}\frac{BK^*}{m}\left(p^\beta (r_P)^{\beta'} + p^{\beta'}(r_P)^\beta\right)\Gamma^{\alpha\alpha'}. \quad (22)$$

Here

$$\Gamma^{\alpha\alpha'} = p^\alpha \epsilon^{\alpha'\gamma\delta\rho} p_\gamma (r_P)_\delta (s_p)_\rho + p^{\alpha'}\epsilon^{\alpha\gamma\delta\rho} p_\gamma (r_P)_\delta (s_p)_\rho. \quad (23)$$

The function A_t is asymmetric in the indices

$$A_t^{\alpha\alpha';\beta\beta'} = 2\mathrm{i}|t|\frac{B^*K}{m}\Big[p^\alpha p^\beta \epsilon^{\alpha'\beta'\delta\rho} p_\delta (s_p)_\rho + p^\alpha p^{\beta'}\epsilon^{\alpha'\beta\delta\rho} p_\delta (s_p)_\rho + p^{\alpha'} p^\beta \epsilon^{\alpha\beta'\delta\rho} p_\delta (s_p)_\rho + p^{\alpha'} p^{\beta'} \epsilon^{\alpha\beta\delta\rho} p_\delta (s_p)_\rho\Big]. \quad (24)$$

Note that these forms are general and can be used for different polarization vectors of the proton. For longitudinal proton polarization, the structure D should be considered in addition.

4 Diffractive vector meson leptoproduction

Now we proceed to analyze the amplitude of vector meson production through the photon–two-gluon fusion. In what follows, we will mainly consider the J/Ψ meson production. This meson can be considered as an S-wave system of heavy $c\bar{c}$ quarks [35]. The J/Ψ-wave function in this case has the form

$$\Psi_V = g(\not{k} + m_q)\gamma_\mu \quad (25)$$

where k is the momentum of a quark, and m_q is its mass. In the non-relativistic approximation, both quarks have momenta k equal to half of the vector meson momentum K_J, and the mass of the c quark is equal to $m_J/2$. The transverse quark motion is not considered. This means that the vector meson distribution amplitude is approximated by the simple form $\delta(\tau - 1/2)\delta(k_t^2)$. The constant

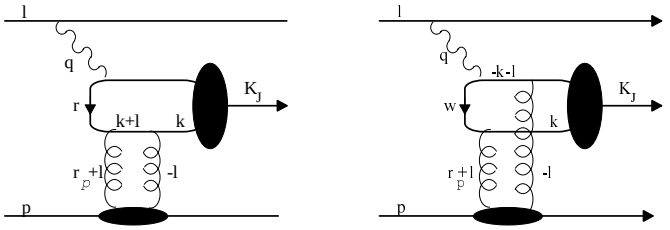

(a) (b)

Fig. 2a,b. Two-gluon contribution to diffractive vector meson production

g in the wave function can be expressed through the e^+e^- decay width of the J/Ψ meson [10]:

$$g^2 = \frac{3\Gamma^J_{e^+e^-} m_J}{64\pi\alpha^2}. \tag{26}$$

The leading twist wave function (25) produces both amplitudes with longitudinal and transverse vector meson polarization because of non-zero mass m_q. For the light meson production $m_q = 0$, and one must consider the higher twist effects to calculate the amplitude with transverse vector meson polarization (see e.g. [18]).

It is known (see e.g. [10,11]) that the leading terms of the amplitude of diffractive vector meson production is mainly imaginary. We shall consider here only the imaginary parts of the amplitudes. In this case, only the graphs of Fig. 2 contribute. The gluons are coupled with single and different quarks in the $c\bar{c}$ loop (see Fig. 2a,b). To calculate the imaginary part of the amplitude, we should consider the δ function contribution in the s-channel propagators ($k + l$ and $p' - l$ lines for Fig. 2a). With the help of δ functions the integration over l

$$\int \mathrm{d}^4 l = \frac{1}{2}\int \mathrm{d}l_+ \mathrm{d}l_- \mathrm{d}l_\perp \tag{27}$$

can be carried out over the l_+ and l_- variables. One can find that the $l_\pm$ components of the vector l both are small: $l_+ \sim l_- \propto 1/p_+$. This results in the transverse character of the gluon momentum $l^2 \simeq -l^2_\perp$. The same is true for integration over l in the non-planar graph of Fig. 2b. For the arguments in the off mass-shell quark propagators of Fig. 2a,b, we find

$$\begin{aligned} r^2 - m_q^2 &= -\frac{M_J^2 + Q^2 + |t|}{2}, \\ w^2 - m_q^2 &= -2\left(l_\perp^2 + \vec{l}_\perp \vec{r}_\perp + \frac{M_J^2 + Q^2 + |t|}{4}\right). \end{aligned} \tag{28}$$

Thus, these quark lines are far from the mass shell for heavy vector meson production even for small Q^2 [10].

In what follows we calculate the polarized cross section of vector meson production. The cross section can be represented as the square of the $\gamma^\star g g \to V$ amplitude convoluted with the lepton and hadron polarized tensors. Some details of the calculations conducted for longitudinal target polarization can be found in [36].

We consider both longitudinal and transverse polarization of the vector meson which can be carried out directly for J/Ψ production for the wave function (25). For the sum over the polarization of the J/Ψ polarized vectors e_J we have

$$\sum_{\mathrm{Spin}_J} e_J^\rho (e_J^\sigma)^+ = -g^{\rho\sigma} + \frac{K_J^\rho K_J^\sigma}{m_J^2}. \tag{29}$$

The spin-averaged and spin-dependent cross sections of vector meson leptoproduction with longitudinal polarization of a lepton and transverse polarization of the proton are determined by the relation

$$\mathrm{d}\sigma(\pm) = \frac{1}{2}\left(\mathrm{d}\sigma(\rightarrow\Downarrow) \pm \mathrm{d}\sigma(\rightarrow\Uparrow)\right). \tag{30}$$

The cross section $\mathrm{d}\sigma(\pm)$ can be written in the form

$$\frac{\mathrm{d}\sigma^\pm}{\mathrm{d}Q^2 \mathrm{d}y \mathrm{d}t} = \frac{|T^\pm|^2}{32(2\pi)^3 Q^4 s^2 y}. \tag{31}$$

For the spin-averaged amplitude squared we find

$$\begin{aligned} |T^+|^2 = \frac{s^2 N}{4\bar{Q}^4}&\left((1+(1-y)^2)m_V^2 + 2(1-y)Q^2\right) \\ &\times \left[|\tilde{B}|^2 + |\tilde{K}|^2 \frac{|t|}{m^2}\right]. \end{aligned} \tag{32}$$

Here $\bar{Q}^2 = (m_V^2 + Q^2 + |t|)/4$, and N is the normalization factor

$$N = \frac{\Gamma^J_{e^+e^-} M_J \alpha_s^4}{27\pi^2}. \tag{33}$$

The term proportional to $(1+(1-y)^2)m_V^2$ in (32) represents the contribution of the virtual photon with transverse polarization. The $2(1-y)Q^2$ term describes the effect of longitudinal photons. This contribution is predominant for high Q^2. The $\tilde{B}$ and $\tilde{K}$ functions are expressed through the integral over the transverse momentum of the gluon. The function $\tilde{B}$ is determined by

$$\begin{aligned} \tilde{B} = \ & \bar{Q}^2 \int \frac{\mathrm{d}^2 l_\perp (l_\perp^2 + \vec{l}_\perp \vec{r}_\perp) B(t, l_\perp^2, x_P, \cdots)}{(l_\perp^2 + \lambda^2)((\vec{l}_\perp + \vec{\Delta})^2 + \lambda^2)[l_\perp^2 + \vec{l}_\perp \vec{r}_\perp + \bar{Q}^2]} \\ &\sim \int_0^{l_\perp^2 < \bar{Q}^2} \frac{\mathrm{d}^2 l_\perp (l_\perp^2 + \vec{l}_\perp \vec{r}_\perp)}{(l_\perp^2 + \lambda^2)((\vec{l}_\perp + \vec{r}_\perp)^2 + \lambda^2)} B(t, l_\perp^2, x_P, \cdots). \end{aligned} \tag{34}$$

We find that the cross sections depend on the variable $\bar{Q}^2$ which is a modification of the scale variable proposed in [10,11] for the case of large momentum transfer. The term $(l_\perp^2 + \vec{l}_\perp \vec{r}_\perp)$ appears in the numerator of (34) because of the cancellation between the planar and non-planar graphs where the gluons are coupled with single and different quarks (Fig. 2). The $\tilde{K}$ function is determined by a similar integral. The integral (34) can be connected with the gluon SPD:

$$\begin{aligned} &\mathcal{F}^g_{x_P}(x_P, t, \bar{Q}^2) \\ &\sim \int_0^{l_\perp^2 < \bar{Q}^2} \frac{\mathrm{d}^2 l_\perp (l_\perp^2 + \vec{l}_\perp \vec{r}_\perp)}{(l_\perp^2 + \lambda^2)((\vec{l}_\perp + \vec{r}_\perp)^2 + \lambda^2)} B(t, l_\perp^2, x_P, \cdots) \\ &= \tilde{B}. \end{aligned} \tag{35}$$

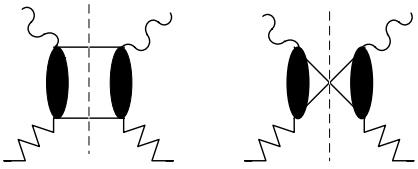

Fig. 3. Box graphs contributions to the cross section of diffractive $Q\bar{Q}$ production

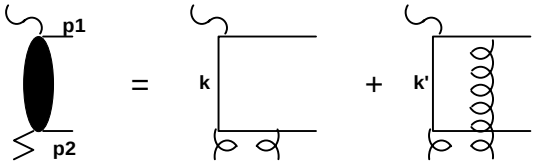

Fig. 4. The amplitude of photon–two-gluon fusion

Note that if one considers the effects of the transverse quark motion in the vector meson wave function, the scale variable in SPD will be changed to $\bar{Q}^2 \to \bar{Q}^2 + k_\perp^2$ [13, 37]. Thus, the $B(l_\perp^2, x_P, \cdots)$ function is a non-integrated spin-averaged gluon distribution. The $\tilde{K}$ function is proportional to the $\mathcal{K}^g_{x_P}(x_P, t)$ distribution. The function ϕ in (14) has the form

$$\phi(l_\perp, \cdots) = \frac{(l_\perp^2 + \vec{l}_\perp \vec{r}_\perp)}{(l_\perp^2 + \lambda^2)((\vec{l}_\perp + \vec{r}_\perp)^2 + \lambda^2)}. \qquad (36)$$

The spin-dependent amplitude squared looks like

$$|T^-|^2 = \frac{\vec{Q}\vec{S}_\perp}{4m} \frac{s|t|N}{4\bar{Q}^4} \left(Q^2 + m_V^2 + |t|\right) \frac{\tilde{B}\tilde{K}^* + \tilde{B}^*\tilde{K}}{2}. \quad (37)$$

We shall use the spin-dependent cross sections obtained here for the numerical analysis of polarized vector meson production in Sect. 6.

5 Diffractive $Q\bar{Q}$ photoproduction

Let us study now the diffractive $Q\bar{Q}$ production in the lepton–proton reaction. This process is determined by graphs similar as shown in Fig. 2. The change is in the photon–two-gluon fusion amplitude where we do not project the $Q\bar{Q}$ state onto the vector meson. The quark–antiquark contribution, instead of t-channel gluons, is possible for light quark production. To suppress this contribution of the quark structure function which should be essential at large x, we investigate quark production at small $x \leq 0.1$. In this kinematical region the gluon contribution is predominant.

As in the case of vector meson production, we calculate the spin-averaged and spin-dependent cross section (31) of diffractive $Q\bar{Q}$ leptoproduction. To calculate these cross sections, we should integrate the corresponding amplitudes squared over the $Q\bar{Q}$ phase space $\mathrm{d}N_{Q\bar{Q}} = \mathit{\Pi}_f \mathrm{d}^3 p_f/((2\pi)^3 2E_f)$ with the delta function that reflects the momentum conservation. It can easily be seen that

$$\frac{\mathrm{d}^3 p_1}{2E_1} \frac{\mathrm{d}^3 p_2}{2E_2} \delta^4(q + r_P - p_1 - p_2) = \mathrm{d}^4 p_1 \delta(p_1^2 - m_q^2) \delta(p_2^2 - m_q^2), \qquad (38)$$

and the calculation of the $\gamma g g \to Q\bar{Q}$ cross section is equivalent to computation of the imaginary part of the quark-loop diagram shown in Fig. 3. The amplitude of photon–two-gluon fusion shown by blobs in Fig. 3 represents a sum of graphs in Fig. 4. The diagrams of Fig. 4 are similar to the planar and non-planar gluon graphs of Fig. 2. As a result, the gluon contribution to the cross section should be similar to that obtained in (34).

The final quark momenta p_1, p_2 and the momentum of the off mass-shell quark k (k') can be determined with the help of delta functions in (38). There are two integration regions for the k vectors. For Region I, we find that $p_1 \sim q$ and $p_2 \sim r_P$,

$$\begin{aligned} p_1 \sim \Bigg(& y p_+ - \frac{|t|}{p_+} - \frac{m_q^2 + (\vec{r}_\perp + \vec{k}_\perp)^2}{p_+ x_P}, \\ & \frac{m_q^2 + (\vec{q}_\perp - \vec{k}_\perp)^2}{p_+ y}, (\vec{q}_\perp - \vec{k}_\perp) \Bigg), \\ p_2 \sim \Bigg(& \frac{m_q^2 + (\vec{r}_\perp + \vec{k}_\perp)^2}{p_+ x_P}, \\ & x_P p_+ - \frac{Q^2}{p_+} - \frac{m_q^2 + (\vec{q}_\perp - \vec{k}_\perp)^2}{p_+ y}, (\vec{r}_\perp + \vec{k}_\perp) \Bigg), \end{aligned} \qquad (39)$$

and the vector k is mainly transverse: $k^2 \sim -k_\perp^2$. The t-channel gluon contribution is predominated if both quark–proton energies are large. We find that

$$(p_1 + p)^2 \sim y p_+^2, \quad (p_2 + p)^2 \sim \frac{m_q^2 + k_\perp^2}{x_P}. \qquad (40)$$

Thus, x_P should be quite small ($x_P \leq 0.1$). At the same time $k_\perp^2$ should not be small (we shall use $k_\perp^2 > 1\,\mathrm{GeV}^2$). A non-small value for k^2 produces the large quark virtuality for the graphs of Fig. 4.

For Region II, the quark momentum interchanged places, $p_1 \leftrightarrow p_2$. In this case, the vector k has a large longitudinal component, and $k^2 \sim -x_P p_+^2$. One can suppose that such contributions should be suppressed. However, in this case, we find a similar large variable from the trace in the numerator of the diagram that compensates p_+^2 in the denominator. A similar compensation between the numerator and denominator takes place for the non-planar quark-loop diagrams (the second graph in Fig. 3). In this case, we have a large variable only in one propagator. The calculation of the $\gamma g g \to Q\bar{Q}$ process is more complicated than the vector meson case. We must consider here eight graphs with two regions for the quark momenta. This generates a complete set of graphs of $Q\bar{Q}$ production.

The integration over the quark momenta $k_\pm$ in the loop can be carried out with the help of delta functions in (38):

$$\mathrm{d}^4k\delta(p_1^2-m_q^2)\delta(p_2^2-m_q^2)\sim\frac{\mathrm{d}^2k_\perp}{M_X^2\sqrt{1-4(k_\perp^2+m_q^2)/M_X^2}}. \tag{41}$$

As a result, the spin-averaged and spin-dependent cross section can be written in the form

$$\frac{\mathrm{d}^5\sigma(\pm)}{\mathrm{d}Q^2\mathrm{d}y\mathrm{d}x_p\mathrm{d}t\mathrm{d}k_\perp^2}=\begin{pmatrix}(2-2y+y^2)\\(2-y)\end{pmatrix}\times\frac{C(x_P,Q^2)N(\pm)}{\sqrt{1-4(k_\perp^2+m_q^2)/M_X^2}}. \tag{42}$$

Here $C(x_P,Q^2)$ is a normalization function which is common for the spin-averaged and spin-dependent cross section; $N(\pm)$ is determined by a sum of the graphs in Figs. 3 and 4 integrated over the gluon momenta l and l':

$$N(\pm)=\int\frac{\mathrm{d}^2l_\perp\mathrm{d}^2l'_\perp(l_\perp^2+\vec{l}_\perp\vec{r}_\perp)\,((l'_\perp)^2+\vec{l}'_\perp\vec{r}_\perp)}{(l_\perp^2+\lambda^2)((\vec{l}_\perp+\vec{r}_\perp)^2+\lambda^2)}\times\frac{D^\pm(t,Q^2,l_\perp,l'_\perp,\cdots)}{(l'^2_\perp+\lambda^2)((\vec{l}'_\perp+\vec{r}_\perp)^2+\lambda^2)}. \tag{43}$$

The $D^\pm$ function here is a sum of traces over the quark loops of the graphs in Figs. 3 and 4 convoluted with the spin-averaged and spin-dependent tensors. The calculation shows a considerable cancellation between the planar and non-planar contribution of the graphs in Fig. 4. As a result, in the numerator of (43) we find the terms proportional to the gluon momenta $l_\perp$ and $l'_\perp$ as in the case of vector meson production (34).

For simplicity we write the analytic forms of the graph contribution to the cross sections in the limit $\beta\to 0$. The numerical calculation will be fulfiled for arbitrary β. The contribution of the sum of the graphs of Figs. 3 and 4 to the D^+ function for Region I can be written in the form

$$D_I^+=\frac{Q^2\left(|B|^2+|t|/m^2|K|^2\right)\left((k_\perp+r_\perp)^2+m_q^2\right)}{\left(k_\perp^2+m_q^2\right)\left((k_\perp-l_\perp)^2+m_q^2\right)\left((k_\perp-l'_\perp)^2+m_q^2\right)}. \tag{44}$$

This function contains a product of the off mass-shell quark propagators in the graphs of Fig. 3 and 4. We see that the quark virtuality here is quite different as compared to the vector meson case. We have no terms proportional to Q^2 as in (28).

This will change the scale in the corresponding gluon structure functions. In fact, the denominators in (44) determine the effective integration region over l and l' in (33). We can approximately rewrite the contribution of $D^p(+)$ to $N(+)$

$$N^p(+)\sim\frac{\left(|\tilde{B}|^2+|t|/m^2|\tilde{K}|^2\right)\left((k_\perp+r_\perp)^2+m_q^2\right)}{\left(k_\perp^2+m_q^2\right)^3}, \tag{45}$$

with

$$\tilde{B}\sim\int_0^{l_\perp^2<k_0^2}\frac{\mathrm{d}^2l_\perp(l_\perp^2+\vec{l}_\perp\vec{r}_\perp)}{(l_\perp^2+\lambda^2)((\vec{l}_\perp+\vec{r}_\perp)^2+\lambda^2)}B(t,l_\perp^2,x_P,\cdots)=\mathcal{F}^g_{x_P}(x_P,t,k_0^2) \tag{46}$$

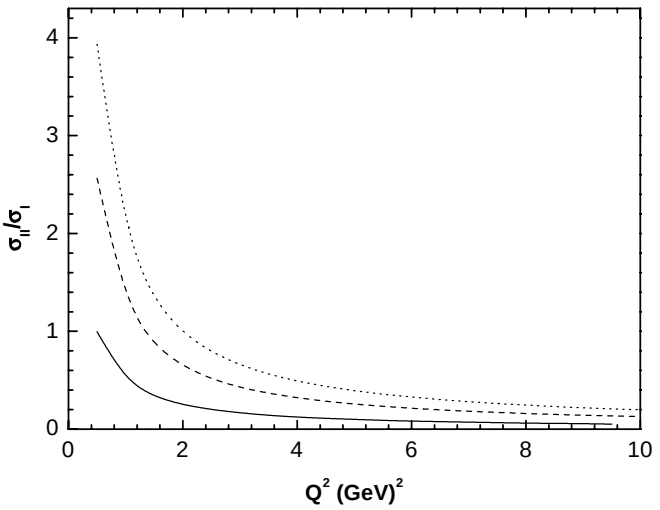

Fig. 5. The ratio of cross sections for Regions II and I at $s^{1/2}=20\,\mathrm{GeV}$ for $x_P=0.1$, $y=0.5$, $|t|=0.3\,\mathrm{GeV}^2$: the solid line is for $k^2=1\,\mathrm{GeV}^2$, the dashed line for $k^2=3\,\mathrm{GeV}^2$, the dotted line for $k^2=5\,\mathrm{GeV}^2$

and

$$\tilde{K}\sim\int_0^{l_\perp^2<k_0^2}\frac{\mathrm{d}^2l_\perp(l_\perp^2+\vec{l}_\perp\vec{r}_\perp)}{(l_\perp^2+\lambda^2)((\vec{l}_\perp+\vec{r}_\perp)^2+\lambda^2)}K(t,l_\perp^2,x_P,\cdots)=\mathcal{K}^g_{x_P}(x_P,t,k_0^2), \tag{47}$$

with $k_0^2\sim k_\perp^2+m_q^2$. For non-zero β this scale is changed to $k_0^2\sim(k_\perp^2+m_q^2)/(1-\beta)$ and coincides with that found in [21,22]. As we expected, the gluon structure functions are determined by the same integrals as in (35) but on a different scale.

For Region II, only the first planar graph of Fig. 3 contributes. As a result of the compensation of the gluon contributions shown in Fig. 4, the form (43) is valid here too. The graphs here have lines with large quark virtuality. Propagators of these lines become pointlike. As a result, the contribution to the cross section for Region II has different Q^2 and k^2 dependences with respect to Region I. We find

$$D_{\mathrm{II}}^+=\frac{2(1-y)\left(|B|^2+|t|/m^2|K|^2\right)}{(2-2y+y^2)\left((k_\perp+r_\perp)^2+m_q^2\right)}. \tag{48}$$

The ratio of the cross sections for Regions I and II is shown in Fig. 5. The ratio is growing with k^2. We find that the integration region II is essential at small Q^2. It can be seen that the contribution of the D functions (44) and (48) to the cross section (42) is proportional to $D_{\mathrm{I}}^+\propto(2-2y+y^2)$, $D_{\mathrm{II}}^+\propto 2(1-y)$. They represent, as in (32), the contributions with transverse and longitudinal photon polarization, respectively [21].

The contribution of all graphs to the function $N(+)$ can be written as

$$N(+)=\left(|\tilde{B}|^2+|t|/m^2|\tilde{K}|^2\right)\Pi^{(+)}(t,k_\perp^2,Q^2). \tag{49}$$

The function $\Pi^{(+)}$ for non-zero β is complicated in form and will be calculated numerically.

The same procedure is used in calculations of the spin-dependent cross sections. The spin-dependent leptonic and hadronic tensors (10) and (20) are used in this case. The spin-dependent part of the hadronic tensor (20) is much more complicated than the one of (17). This results in tangled analytic expressions of the spin-dependent cross sections. We shall discuss here only the general structure of this observable. In addition to the term observed in (37) and proportional to the scalar product $\vec{Q}\vec{S}_\perp$, the new term $\propto \vec{k}_\perp\vec{S}_\perp$ appears. As a result, we find the following representation of the function $N(-)$:

$$N(-) = \sqrt{\frac{|t|}{m^2}}\left(\tilde{B}\tilde{K}^* + \tilde{B}^*\tilde{K}\right) \times \left[\frac{(\vec{Q}\vec{S}_\perp)}{m}\Pi_Q^{(-)}(t,k_\perp^2,Q^2) + \frac{(\vec{k}_\perp\vec{S}_\perp)}{m}\Pi_k^{(-)}(t,k_\perp^2,Q^2)\right]. \quad (50)$$

The second term in (50) cannot be found in the vector meson production, because we should integrate there the amplitudes over $\mathrm{d}^2k_\perp$. The functions $\Pi^{(-)}_{Q(k)}$ will be calculated numerically like the function $\Pi^{(+)}$.

6 Numerical results for vector meson leptoproduction

We shall calculate the polarized cross section (30) of diffractive J/Ψ production determined by the amplitudes (32) and (37). The spin-averaged cross section of the vector meson production at a small momentum transfer is proportional to the $|\tilde{B}|^2$ function (32) which is connected with the skewed gluon distribution (35). This result is in accordance with the imaginary part of the amplitude found on the basis of the SPD approach [1]. We use here a simple parameterization of the SPD, a product of the form factor and the ordinary gluon distribution:

$$\tilde{B}(t,x_P,\bar{Q}^2) = F_B(t)\left(x_P G(x_P,\bar{Q}^2)\right), \quad (51)$$

where for simplicity the form factor $F_B(t)$ is chosen as the electromagnetic form factor of the proton. Such a simple choice can be justified by the fact that the pomeron–proton vertex might be similar to the photon–proton coupling [38,39]

$$F_B(t) \sim F_p^{\mathrm{em}}(t) = \frac{(4m_p^2 + 2.8|t|)}{(4m_p^2+|t|)(1+|t|/0.7\,\mathrm{GeV}^2)^2}. \quad (52)$$

To perform simple estimations, we shall use our results from [30,32] where it was found that the ratio of spin asymmetries in exclusive reactions at small momentum transfer may have a weak energy dependence. The corresponding asymmetries are proportional to the ratio $|\tilde{K}|/|\tilde{B}|$ at small $x \sim 1/s$. We shall suppose that this is true for the ratio of spin-dependent and spin-averaged densities in our case too and

$$\frac{|\tilde{K}|}{|\tilde{B}|} \sim 0.1. \quad (53)$$

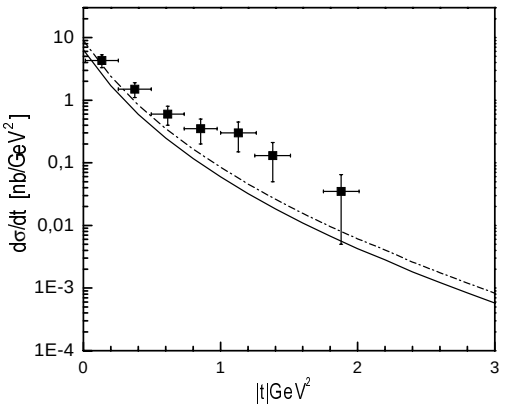

Fig. 6. The differential cross section of J/Ψ production at HERA energy: the solid line is for $|\tilde{K}|/|\tilde{B}| = 0$, the dot-dashed line for $|\tilde{K}|/|\tilde{B}| = 0.1$. Data are from [6]

We shall use this value in our estimation of the spin asymmetries of hadron leptoproduction at small x.

The energy dependence of the cross sections is determined by the pomeron contribution to the gluon distribution function at small x,

$$\left(x_P G(x_P,\bar{Q}^2)\right) \sim \frac{\mathrm{const}}{x_P^{\alpha_p(t)-1}} \sim \left(\frac{sy}{m_J^2+Q^2+|t|}\right)^{(\alpha_p(t)-1)}. \quad (54)$$

Here $\alpha_p(t)$ is a pomeron trajectory which is chosen in the form

$$\alpha_p(t) = 1 + \epsilon + \alpha' t. \quad (55)$$

with $\epsilon = 0.15$ and $\alpha' = 0$. These values are in accordance with the fit of diffractive J/Ψ production by ZEUS [40]

The typical scale of the reaction is determined by $\bar{Q}^2 = (m_J^2 + Q^2 + |t|)/4$. For Q^2 and $|t|$ not large, the value of $\bar{Q}^2$ is about 2.5–3.0 GeV^2. In this region, we can work with fixed $\alpha_\mathrm{s} \sim 0.3$. The effective gluon mass in (34) is chosen to be equal to $0.3\,\mathrm{GeV}^2$. The cross section weakly depends on this parameter. The value of $\Gamma^J_{e^+e^-} = 5.26\,\mathrm{keV}$ is used. The predicted cross sections are shown in Fig. 6. Our results reproduce the experimental data quite well.

The $A_{l\mathrm{T}}$ asymmetry for vector meson production is determined by the ratio of cross sections determined in (37) and (32):

$$A_{l\mathrm{T}} = \frac{\sigma(-)}{\sigma(+)} \sim \frac{\vec{Q}\vec{S}_\perp}{4m}\frac{yx_P|t|}{(1+(1-y)^2)m_V^2 + 2(1-y)Q^2} \times \frac{\tilde{B}\tilde{K}}{|\tilde{B}|^2 + |\tilde{K}|^2|t|/m^2}. \quad (56)$$

For small momentum transfer, this asymmetry can be approximated by

$$A_{l\mathrm{T}} \sim C_g \frac{\mathcal{K}^g_\zeta(\zeta)}{\mathcal{F}^g_\zeta(\zeta)} \quad \text{with } \zeta = x_P. \quad (57)$$

Simple estimations show that the coefficient $C_g(J/\Psi)$ at a HERMES energy for $y = 0.5$, $|t| = 1\,\mathrm{GeV}^2$, $Q^2 = 5\,\mathrm{GeV}^2$

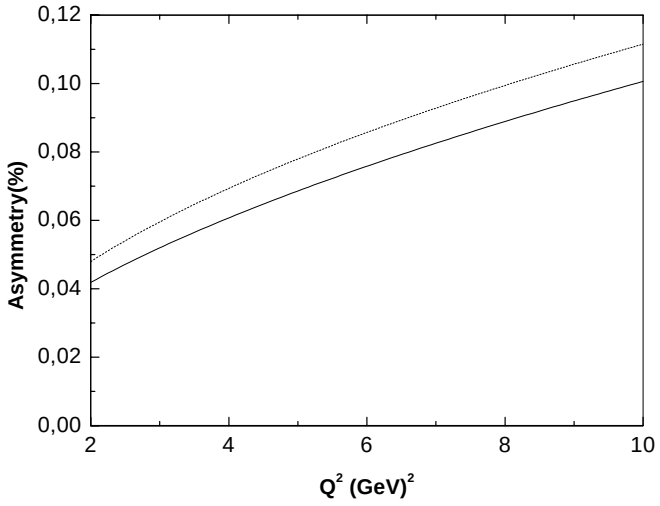

Fig. 7. The $A_{l\mathrm{T}}$ asymmetry for vector meson production at $s^{1/2} = 7\,\mathrm{GeV}$ ($y = 0.5$, $|t| = 1\,\mathrm{GeV}^2$): the solid line is for J/Ψ production, the dotted line for ρ production

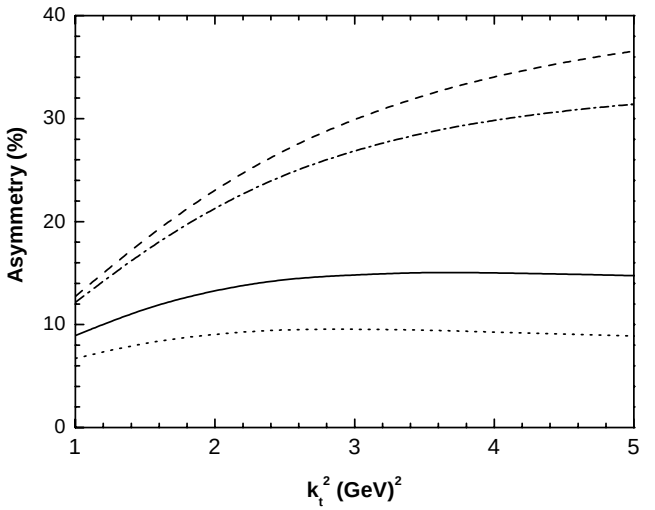

Fig. 8. The $A^k_{l\mathrm{T}}$ asymmetry in diffractive light $Q\bar{Q}$ production at $s^{1/2} = 20\,\mathrm{GeV}$ for $x_P = 0.1$, $y = 0.5$, $|t| = 0.3\,\mathrm{GeV}^2$: the dotted line for $Q^2 = 0.5\,\mathrm{GeV}^2$, the solid line is for $Q^2 = 1\,\mathrm{GeV}^2$, the dot-dashed line for $Q^2 = 5\,\mathrm{GeV}^2$, the dashed line for $Q^2 = 10\,\mathrm{GeV}^2$

is quite small, about 0.007. To get the expected values for the coefficients (57) for light vector mesons, we use the same equation, (56). The simple model used for the wave function predicts a weak mass dependence of the gluon contribution to the asymmetry. For the same kinematical variables, $C(\phi) \sim C(\rho) \sim 0.008$. However, these results are obtained for the non-relativistic meson wave function of the form $\delta(\tau - 1/2)\delta(k_t^2)$, which is not a good approximation for light meson production. To get suitable predictions for ρ, ϕ meson production, it is important to study a more realistic wave function and take into consideration the transverse quark degrees of freedom. Moreover, for ρ, ϕ meson production, the contribution of the quark SPD should be considered in the HERMES energy range.

The asymmetry predicted for J/Ψ production at HERMES energies is shown in Fig. 7 ($\tilde{K}/\tilde{B} = 0.1$) for the case when the transverse part of the photon momentum is parallel to the target polarization $S_\perp$. Simple estimations on the basis of (57) for ρ meson production are shown there too. At the HERA energies, the asymmetry will be extremely small.

7 Predictions for $Q\bar{Q}$ leptoproduction

We shall discuss here our prediction for polarized diffractive $Q\bar{Q}$ production. We do not consider the cross section but only the asymmetry $A_{l\mathrm{T}} = \sigma(-)/\sigma(+)$. In estimations we shall use the same parameterizations of SPD as in (51) with the functions determined in (52). As in the case of vector meson production, the asymmetry is approximately proportional to the ratio of polarized and spin-averaged gluon distribution functions,

$$A_{l\mathrm{T}}^{Q\bar{Q}} \sim C^{Q\bar{Q}} \frac{\mathcal{K}^g_\zeta(\zeta)}{\mathcal{F}^g_\zeta(\zeta)} \quad \text{with } \zeta = x_P. \tag{58}$$

As previously, in our estimations we use the value $|\tilde{K}|/|\tilde{B}| \sim 0.1$.

The spin-dependent contribution has two terms proportional to the scalar products $\vec{k}_\perp \vec{S}_\perp$ and $\vec{Q}\vec{S}_\perp$ (50). We shall study these contributions to the asymmetry separately. The first term will be analyzed for the case when the transverse jet momentum $\vec{k}_\perp$ is parallel to the target polarization $\vec{S}_\perp$. The asymmetry is maximal in this case. We would like to emphasize here that to observe this contribution to the asymmetry, it is necessary to distinguish experimentally between quark and antiquark jets. This can be realized presumably by the charge of the leading particles in the jet which should be connected in charge with the quark produced in photon–gluon fusion. This is an indispensable condition in the experimental study of that asymmetry caused by the fact that the transverse momentum of a quark and an antiquark produced in the process are opposite in sign. If we do not separate events with $\vec{k}_\perp$ for the quark jet e.g., the resulting asymmetry will be zero.

The spin-dependent cross section vanishes for $Q^2 \to 0$, while the spin-averaged cross section is constant in this limit. As a result, the asymmetry can be estimated as $A_{l\mathrm{T}} \propto Q^2/(Q^2 + Q_0^2)$ with $Q_0^2 \sim 1\,\mathrm{GeV}^2$. The Q^2 dependence of the asymmetry for light quark production at energy $s^{1/2} = 20\,\mathrm{GeV}$ is shown in Fig. 8. The predicted asymmetry for heavy $c\bar{c}$ production is approximately of the same order of magnitude (see Fig. 9).

At the energy $s^{1/2} = 7\,\mathrm{GeV}$ (HERMES) it is not so easy to study the perturbative region for $Q\bar{Q}$ production. In fact, $k_\perp^2$ should be large enough to have a large scale k_0^2 in the process (47). Otherwise, from (41), we have the restriction that $k^2 \le M_X^2/4$. In this energy range for quite large $M_X^2 \sim (8\text{–}10)\,\mathrm{GeV}^2 \sim M_{J/\Psi}^2$ we find that $(k_\perp^2)_{\max} \sim 2\,\mathrm{GeV}^2$. This means that we can work only in a very limited region of k^2. The expected $A_{l\mathrm{T}}$ asymmetry for light quark production at HERMES is shown in Fig. 10.

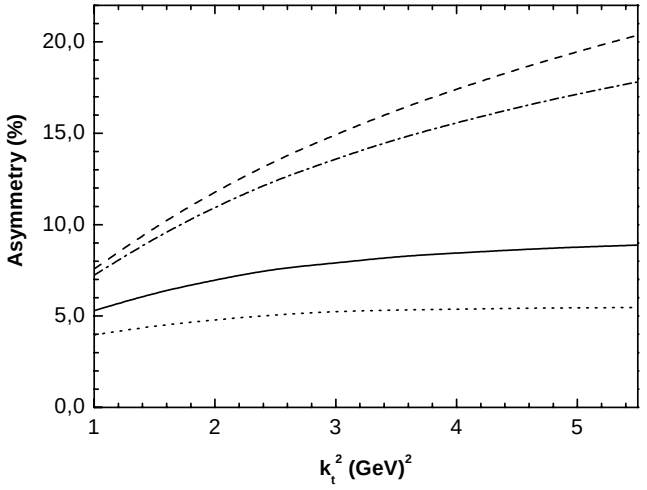

Fig. 9. The $A_{l\mathrm{T}}^{k}$ asymmetry in diffractive heavy $Q\bar{Q}$ production at $s^{1/2} = 20\,\mathrm{GeV}$ for $x_P = 0.1$, $y = 0.5$, $|t| = 0.3\,\mathrm{GeV}^2$: the dotted line is for $Q^2 = 0.5\,\mathrm{GeV}^2$, the solid line for $Q^2 = 1\,\mathrm{GeV}^2$, the dot-dashed line for $Q^2 = 5\,\mathrm{GeV}^2$, the dashed line for $Q^2 = 10\,\mathrm{GeV}^2$

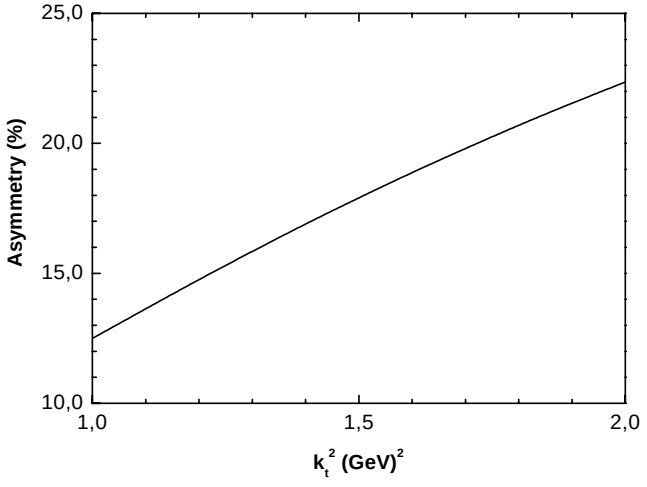

Fig. 10. The $A_{l\mathrm{T}}^{k}$ asymmetry in diffractive light $Q\bar{Q}$ production for $Q^2 = 5\,\mathrm{GeV}^2$, $x_P = 0.1$, $y = 0.5$, $|t| = 0.3\,\mathrm{GeV}^2$ at $s^{1/2} = 7\,\mathrm{GeV}$

We find that for $k_\perp^2 = 1.3\,\mathrm{GeV}^2$, $Q^2 = 5\,\mathrm{GeV}^2$, $x_P = 0.1$, $y = 0.5$, and $|t| = 0.3\,\mathrm{GeV}^2$, the coefficient $C_k^{Q\bar{Q}}$ in (58) is quite large, about 1.5 at the HERMES energy. This shows that there is a possibility to study the polarized gluon distribution $\mathcal{K}_\zeta^g(x)$ in the HERMES experiment.

The contribution to the asymmetry $\propto \vec{Q}\vec{S}_\perp$ is simpler to study experimentally. Moreover, this term is connected directly with the diffractive contribution with the $A_\perp$ asymmetry [27]. We shall analyze this term for the case when the transverse jet momentum $\vec{Q}_\perp$ is parallel to the target polarization $\vec{S}_\perp$ (a maximal contribution to the asymmetry). The predicted $A_{l\mathrm{T}}^{Q}$ asymmetry in diffractive light $Q\bar{Q}$ production at $s^{1/2} = 20\,\mathrm{GeV}$ is shown in Fig. 11. This asymmetry is not small for $Q^2 \sim (0.5\text{–}1)\,\mathrm{GeV}^2$. In contrast to the $A_{l\mathrm{T}}^{k}$ term, the $A_{l\mathrm{T}}^{Q}$ asymmetry has a strong

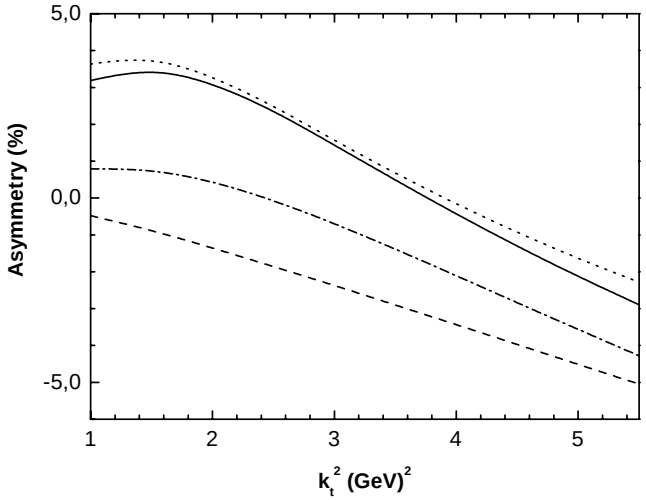

Fig. 11. $A_{l\mathrm{T}}^{Q}$ asymmetry in diffractive light $Q\bar{Q}$ production at $s^{1/2} = 20\,\mathrm{GeV}$ for $x_P = 0.1$, $y = 0.5$, $|t| = 0.3\,\mathrm{GeV}^2$: the dotted line is for $Q^2 = 0.5\,\mathrm{GeV}^2$, the solid line for $Q^2 = 1\,\mathrm{GeV}^2$, the dot-dashed line for $Q^2 = 5\,\mathrm{GeV}^2$, the dashed line for $Q^2 = 10\,\mathrm{GeV}^2$

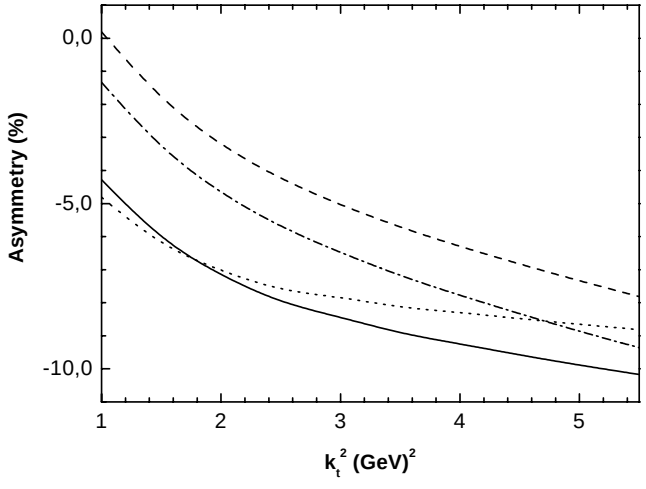

Fig. 12. The $A_{l\mathrm{T}}^{Q}$ asymmetry in diffractive heavy $Q\bar{Q}$ production at $s^{1/2} = 20\,\mathrm{GeV}$ for $x_P = 0.1$, $y = 0.5$, $|t| = 0.3\,\mathrm{GeV}^2$: the dotted line is for $Q^2 = 0.5\,\mathrm{GeV}^2$, the solid line for $Q^2 = 1\,\mathrm{GeV}^2$, the dot-dashed line for $Q^2 = 5\,\mathrm{GeV}^2$, the dashed line for $Q^2 = 10\,\mathrm{GeV}^2$

mass dependence. For heavy quark production, this asymmetry becomes negative; see Fig. 12.

It is interesting to look for what we expect to observe for light quark production at low energy, $s^{1/2} = 7\,\mathrm{GeV}$. The predicted asymmetry for different momentum transfers is shown in Fig. 13. Note that in fixed-target experiments, it is usually difficult to detect the final hadron and determine the momentum transfer. In this case, it will be good to have predictions for the asymmetry integrated over the momentum transfer

$$\bar{A}_{l\mathrm{T}}^{Q} = \frac{\int_{t_{\min}}^{t_{\max}} \sigma(-)\mathrm{d}t}{\int_{t_{\min}}^{t_{\max}} \sigma(+)\mathrm{d}t}. \tag{59}$$

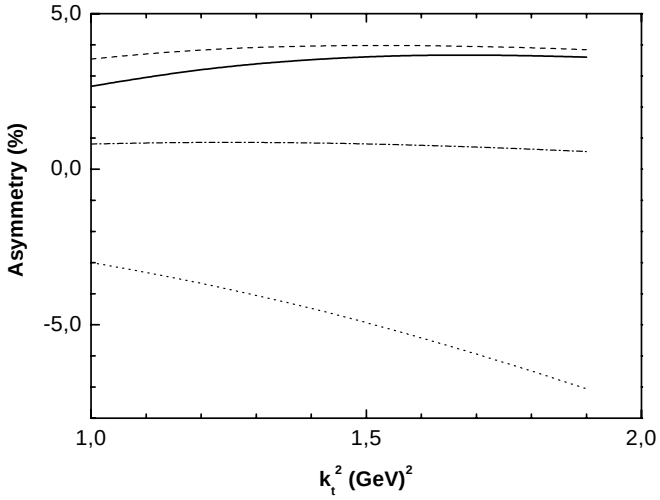

Fig. 13. The $A_{l\mathrm{T}}^{Q}$ asymmetry in diffractive light $Q\bar{Q}$ production at $s^{1/2} = 7\,\mathrm{GeV}$ for $Q^2 = 5\,\mathrm{GeV}^2$, $x_P = 0.1$, $y = 0.5$: the dotted line is for $|t| = 0.1\,\mathrm{GeV}^2$, the dot-dashed line for $|t| = 0.3\,\mathrm{GeV}^2$, the dashed line for $|t| = 0.5\,\mathrm{GeV}^2$, the solid line is for integration over the $|t|$ asymmetry

We integrate cross sections from $t_{\min} \sim (x_P m)^2 \sim 0$ up to $t_{\max} = 4\,\mathrm{GeV}^2$. The predicted integrated asymmetry (see Fig. 13) is not small; about 3%.

8 Conclusion

In the present paper, diffractive hadron leptoproduction for a longitudinally polarized lepton and a transversely polarized proton at high energies has been studied within the two-gluon exchange model. The polarized cross sections of diffractive hadron production are determined in terms of the leptonic and hadronic tensors and the squared amplitude of hadron production through the photon–two-gluon fusion. The hadronic tensor is expressed in terms of the two-gluon couplings with the proton that are related to SPD. As a result, the cross sections of diffractive meson and $Q\bar{Q}$ production are expressed in terms of the same integrals as are connected with the gluon SPD, $\mathcal{F}_\zeta(x)$ and $\mathcal{K}_\zeta(x)$.

The $A_{l\mathrm{T}}$ asymmetry is found to be proportional to the ratio of the $\mathcal{K}/\mathcal{F}$ structure functions and generally can be used to get information on the transverse distribution $\mathcal{K}^g_{x_P}(x_P, t)$ from experiment. The asymmetry of vector meson production is expected to be quite small, $A_{l\mathrm{T}} < 0.1\%$ in the HERMES energy range. This result was obtained for a simple non-relativistic form of the vector meson wave function and generally can be used only for heavy meson production. The $A_{l\mathrm{T}}$ asymmetry for $Q\bar{Q}$ production contains two independent terms which are proportional to the scalar products $\vec{k}_\perp \vec{S}_\perp$ and $\vec{Q}\vec{S}_\perp$ (50). The first one, $\propto \vec{k}_\perp \vec{S}_\perp$, has no x_P suppression and is predicted to be about 10%. It might be an excellent object to study transverse effects in the proton coupling with gluons. However, the experimental study of this asymmetry is not so simple. To find non-zero asymmetry in this case, it is necessary to distinguish quark and antiquark jets and to have a possibility to study the azimuthal asymmetry structure. This is an important condition, because the polarized cross section integrated over $\mathrm{d}\phi_{\mathrm{Jet}}$ is equal to zero. Note that the asymmetry of the same order of magnitude was predicted for diffractive $Q\bar{Q}$ production in polarized proton–proton interaction [41].

The second term $\propto \vec{Q}\vec{S}_\perp$ in the $A_{l\mathrm{T}}$ asymmetry of $Q\bar{Q}$ production is related to the diffractive contribution to the $A_\perp$ asymmetry. The expected asymmetry in this case is not small too. The predicted coefficient $C_Q^{Q\bar{Q}}$ in (58) is about 0.3. This shows the possibility to study the ratio of polarized gluon distributions $\mathcal{K}/\mathcal{F}$ in diffractive $Q\bar{Q}$ leptoproduction. All these results should be applicable to the reactions with heavy quarks. For processes with light quarks, our predictions can be used in the small x region (e.g. $x \leq 0.1$), where the contribution of quark SPD is expected to be small.

Now, we have no the definite predictions for the $A_{l\mathrm{T}}$ asymmetry in light vector meson production. Including the transverse quark motion and higher twist effects for a transversely polarized ρ meson might be important for the asymmetry. In the region of a non-small $x \geq 0.1$ in the HERMES experiments, the polarized quark SPD might be studied together with the gluon distribution in the case of ρ production. In the case of ϕ production, the strange quark SPD might be analyzed. Similar experiments can be conducted at the future COMPASS spectrometer if a transversely polarized target is constructed there.

We conclude that important information on the spin-dependent SPD at small x can be obtained from the asymmetries in diffractive hadron leptoproduction for longitudinally polarized lepton and transversely polarized hadron targets.

Acknowledgements. We would like to thank A. Borissov, A. Efremov, P. Kroll, T. Morii, O. Nachtmann, W.-D. Nowak, and O. Teryaev for fruitful discussions. This work was supported in part by the Russian Foundation for Basic Research, Grant 00-02-16696.

References

1. A.V. Radyushkin, Phys. Rev. D **56**, 5524 (1997)
2. X. Ji, Phys. Rev. D **55**, 7114 (1997)
3. J.C. Collins, L. Frenkfurt, M. Strikman, Phys. Rev. D **56**, 2982 (1997)
4. F.E. Low, Phys. Rev. D **12**, 163 (1975); S. Nussinov, Phys. Rev. Lett. **34**, 1286 (1975)
5. ZEUS Collaboration, J. Breitweg et al., Z. Phys, C **75**, 215 (1997)
6. H1 Collaboration, S. Aid et al., Nucl. Phys. B **472**, 3 (1996)
7. H1 Collaboration, C. Adloff et al., Eur. Phys. J. C **10**, 373 (1999)
8. ZEUS Collaboration, J. Breitweg et al., Eur. Phys. J. C **5**, 41 (1998); H1 Collaboration, C. Adloff et al., Eur. Phys. J. C **6**, 421 (1999)

9. HERMES Collaboration, A. Airapetian et al., Phys. Lett. B **513**, 301 (2001)
10. M.G. Ryskin, Z. Phys. C **57**, 89 (1993)
11. S.J. Brodsky et al., Phys. Rev. D **50**, 3134 (1994)
12. B. Clerbaux, Elastic production of Vector Mesons at HERA: study of the scale of the interaction and measurement of the helicity amplitudes, hep-ph/9908519
13. M.G. Ryskin, R.G. Roberts, A.D. Martin, E.M. Levin, Z. Phys. C **76**, 231 (1997)
14. J.L. Cudell, I. Royen, Nucl. Phys. B **545**, 505 (1999)
15. D.Y. Ivanov, R. Kirshner, Phys. Rev. D **58**, 114026 (1998)
16. L. Mankiewicz, G. Piller, T. Weigl, Eur. Phys. J. C **5**, 119 (1998)
17. H.W. Huang, P. Kroll, Eur. Phys. J. C **17**, 423 (2000)
18. M. Vänttinen, L. Mankiewicz, Phys. Lett. B **434**, 141 (1998)
19. L. Mankiewicz, G. Piller, Phys. Rev. D **61**, 074013 (2000)
20. M. Diehl, Z. Phys. C **66**, 181 (1995)
21. J. Bartels, C. Ewerz, H. Lotter, M. Wüsthoff, Phys. Lett. B **386**, 389 (1996)
22. E.M. Levin, A.D. Martin, M.G. Ryskin, T. Teubner, Z. Phys. C **74**, 671 (1997)
23. B. Lehmann-Dronke, M. Maul, S. Schaefer, E. Stein, A. Schäfer, Phys. Lett. B **457**, 207 (1999)
24. J. Bartels, T. Gehrmann, M.G. Ryskin, Eur. Phys. J. C **11**, 325 (1999)
25. Proceedings of the Topical Workshop Transverse Spin Physics, DESY Zeuthen, July 2001, edited by J. Blümlein, W.-D. Nowak, G. Schnell, Internal Report DESY Zeuthen 01-01 August 2001
26. S.V. Goloskokov, Spin effects in diffractive hadron photoproduction, Proceedings of the 14th International Spin Physics Symposium, SPIN2000, edited by K. Hatanaka, T. Nakano, K. Imai, H. Ejiri, AIP Conference Proceedings V.570, 541; hep-ph/0011341; hep-ph/0110212
27. M. Anselmino, A. Efremov, E. Leader, Phys. Rept. **261**, 1 (1995)
28. M. Anselmino, P. Kroll, B. Pire, Z. Phys. C **36**, 36 (1987)
29. L.V. Gribov, E.M. Levin, M.G. Ryskin, Phys. Rept. **100**, 151 (1983)
30. S.V. Goloskokov, P. Kroll, Phys. Rev. D **60**, 014019 (1999)
31. S.V. Goloskokov, Phys. Lett. B **315**, 459 (1993)
32. S.V. Goloskokov, S.P. Kuleshov, O.V. Selyugin, Z. Phys. C **50**, 455 (1991)
33. D.C. Peaslee et al., Phys. Rev. Lett. **51**, 2359 (1983)
34. N. Akchurin, S.V. Goloskokov, O.V. Selyugin, Int. J. Mod. Phys. A **14**, 253 (1999)
35. E.L. Berger, D. Jones, Phys. Rev. D **23**, 1521 (1981)
36. S.V. Goloskokov, Eur. Phys. J. C **11**, 309 (1999)
37. S.V. Goloskokov, On the $\sigma_{\rm L}/\sigma_{\rm T}$ ratio in polarized vector meson photoproduction. Proceedings of XV International Seminar on High Energy Physics Problems, Relativistic Nuclear Physics and Quantum Chromodynamics, Dubna September 25–29, 2000; hep-ph/0012307
38. A. Donnachie, P.V. Landshoff, Nucl. Phys. B **244**, 322 (1984)
39. T. Arens, M. Diehl, O. Nachtmann, P.V. Landshoff, Z. Phys. C **74**, 651 (1997)
40. ZEUS Collaboration, J. Breitweg et al., Eur. Phys. J. C **14**, 213 (2000)
41. S.V. Goloskokov, Phys. Rev. D **53**, 5995 (1996)